March-April 2020
ISSN: 0193-4120 Page No. 26444 - 26454

Multimodal Biometric Identification using Feature Fusion

Milind Rane, Umesh Bhadade
SSBT's COE&T, Bambhori, Jalgaon, India.

Article Info
Volume 83
Page Number: 26444 - 26454
Publication Issue:
March-April 2020

Article History
Article Received:*12 January 2020*
Revised: *30 January 2020*
Accepted: *15 February 2020*
Publication: *30 April 2020*

Abstract

The Biometric features are already proven to be robust for forensic and security purposes. The fusion of multiple biometric features in a systematic way looks more promising. This paper addresses combining multiple biometric modals using proposed fusion technique with focus on face and palm print features. Five databases are used for experimentation on face, Face94, Face95 and Face96, FERET and FRGC and two dataset used for the palm print, PolyU and IITD database. Transform based features used are extracted from these databases using Gabor transform, Radon transform, Ridgelet transform and Radon-Gabor transform,, FPLBP, TPLBP. Feature level fusion has been applied using algorithms FFVM, FFVW. As per our study accuracy for fusion using TPLBP is 100 %, for FFVW method. Thus, the above feature level fusion technique is recommended, based on better accuracy and robustness

Keywords: *Biometric recognition, human-machine interaction, structural Similarity Index Method (SSIM), Feature level fusion.*

I. Introduction

Digital transactions now a day demands the identification of individuals where privacy of an individual becomes a primary concern to each individual personnel. For every user data privacy or security is of almost important. As due to automation everything is done using digital computers, which are hooked on internet right from automobiles to bank accounts. Entire personal information is accessed through this network and is easily available and is exposed to be misused. Passwords, pin or token (card) are used in automation for access granting, but security provided by these is very weak, as it can be guessed or hacked, and will make available access to some important information on server, mobile or financial accounts, etc. The future technology, Internet of Things (IOT) is susceptible to to risk of confidentiality crack due to attacks on system.

To overcome this diverse and non-alphanumeric method is required to implement, which pointed to the notion of biometric identification [1]. Biometric identification uses biometric traits as one's individual features as a code word, so uses individual face, palmprint, fingerprint, voice etc. for identification. Use of biometric trait is promoted for identification, but flaws like accuracy, variation in trait observed in in these identification systems, which directed to the use of multimodal biometric identification [2].

Multimodal biometrics identification [3] is used in an applications required with high safeguard and of the high pinnacle importance. This improves the false rejection rate (FRR) and, false acceptance rate (FAR) with the variations in biometric traits results in improved true acceptance rate (TAR) i.e. accuracy. Thus, the fusion of two or more than two models of biometrics traits is the identified problem. Multimodal systems are classified based on the fusions technique used for taking decision. The

Published by: The Mattingley Publishing Co., Inc.

March-April 2020
ISSN: 0193-4120 Page No. 26444 - 26454

fusion techniques are score fusion [4], which is based on combination of score levels, feature fusion [5] combines the features of individual biometrics traits, rank fusion [6] based on rank of individual modality and decision fusion [7] which takes decision based on decision of individual biometrics traits. Fusion scheme combines the two modalities of biometrics, by acquiring both from single user and treat each as one entity and use it as the database, as suggested in [2]. The biometrics feature fusion technique requires to select methods which will fuse feature vectors without loss of data and the dimensionality of fused feature vectors need to be moderate.

Majorly identification is done based on confidence based [5] like SSIM [9] which has output value between 0-1 and gives confidence for identification and classification based [8] approach which forms a model based on the fitment of featured training data with ground truth labels.

Different methods of feature extractions are used for face and palm prints identification. These identification methods have less accuracies using unimodal recognition [2], hence, fusion of features is applied for better accuracy and robustness.

The work presented in paper is planned as given below. Literature survey is given and further proposed system is presented. Followed by pre-processing and feature extraction process of database images. Multimodal feature level fusion is proposed, along with experimentation and results are presented. At last conclusions are given and references are cited at the end.

II. LITERATURE SURVEY

All India's Unique Identification Number (UID) project Aadhaar implements the Fusion of Biometric modalities which is using face, iris and fingerprint, all fused together. Scanning of images of iris and face in the absence of adequate lighting conditions may not reveal the exact identification. The above technique pre-dominantly uses L2-norm and Mahalnobis distances. However, this yields better results than single biometric trait. A fusion technique based on features of face image and palmprint is proposed by Yong-Fang Yao et. al. [10], which is based on the normalized weighted feature and classified using nearest neighbor classifier. This results in the accuracy of 90.73%. Raghavendra et al. [11] proposes the fusion technique by concatenating the features of images under query on which particle swarm optimization is applied. The score of individual biometrics modalities are calculated along with the fused feature vector, using these three score fusion is implemented which results in the max accuracy of 97.25% for the FAR of 0.01%.. A concatenated feature fusion is proposed on Gabor filtered image is classified by Kernel DCV-RBF classifier by Xiao-Yuan Jing [12]. The proposed system experimentations are performed on FERET database and HK-PolyU database with max accuracy of 89.90% for two training samples and 92.53% accuracy for three training samples. A matrix based complex feature fusion is proposed by Yong Xu et al. [13]. The accuracy of algorithm found to be 96%. The feature fusion proposed by author [14] by the stack of features of two biometric modalities which results in to accuracy of 98%. But the feature fusion approaches based on concatenating the feature vector struggles with the curse of dimensionality and it becomes even serious with plentiful training samples. Enhanced identification performance can be achieved by mitigating the limitations of above feature fusion.

III. PROPOSED SYSTEM

Figure 1 illustrates the proposed bio-metric identification system which uses multi-modal feature fusion. Raw face images and palmprint images are first acquired. Then the enhancement of these images is carried out for reduction in noise components and improving the contrast of image under query. Furthermore, Region of Interest (ROI) calculation and extraction of face images and palmprint images is done. This is followed by the

Published by: The Mattingley Publishing Co., Inc.

March-April 2020
ISSN: 0193-4120 Page No. 26444 - 26454

feature extraction for ROI of face and palmprints. Feature fusion is implemented based on these extracted features. Identification of person is based on the basis of fused feature set.

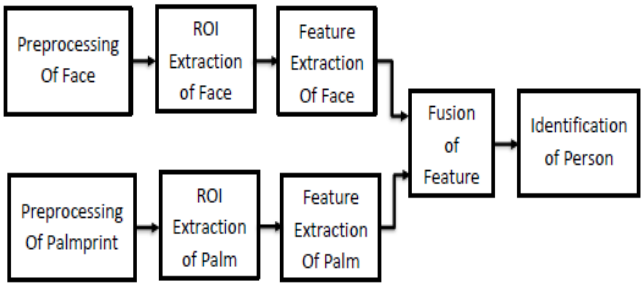

Fig. 1. Block diagram of proposed system

IV. PREPROCESSING

Preprocessing of the data set images plays vital role in the success of recognition systems. Generally, it is used to focus on features of interest and remove unwanted things (like noise, background etc.). Following pre-processing steps are used in this work.

Face ROI Detection and Enhancement

The Face ROI detection and Enhancement block diagram is as given in Figure 2.

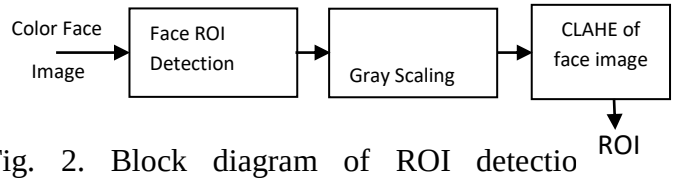

Fig. 2. Block diagram of ROI detectio Enhancement for face image

Face ROI detection [15]

Correct position of face in image acquired is achieved by differentiating image segment into two components viz., face (ROI) or non-face (background of face image). The non-face portion is removed from acquired image. Color of skin in the acquired image is most important for face detection. So, skin color is used to locate face portion in color face images. The steps involved are:

1. Transform an acquired color image into Y, C_b, C_r plane.
2. Binarize the C_r plane of acquired image using threshold of $C_r = 102$
3. Determine the area of regions obtained after binarization. If area of region is greater than 1000 pixels, select the region as Face ROI.
4. Area detected as face region is fitted in bounding box.
5. Acquired image is cropped using the bounding box coordinates.

Gray Scaling [16]

Generally, all the images acquired in databases are colored images. If color information is not necessary, then they are converted into gray scale images for feature extraction and dimensionality reduction (3D matrix to 2D matrix). Since, a single channel is present Luminosity is a weighted average of three basic colors and is given in eq. (1). Sensitivity to green light of human eye is weighted the most being the highest.

$$\text{Im} = \text{Im}(0.21 \times r + 0.72 \times g + 0.07 \times b) \quad (1)$$

Contrast Enhancement:

Although, Adaptive histogram equalization (AHE) [17] improves contrast of image, it also amplifies noise component in similar areas. This necessitates use of Contrast limited adaptive histogram equalization (CLAHE) [18] thereby resolving the noise amplification issue. The sample image and its CLAHE image is shown in Figure 3.

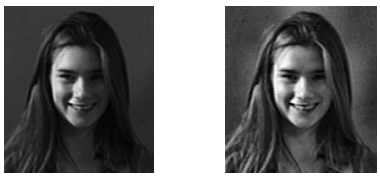

(a) (b)

Fig. 3. (a)Gray scale subject image of faces95. [1] (b)Enhanced image using CLAHE.

Palmprint ROI Detection [19]

Square-based segmentation approach is adopted to detect ROI of Palmprint image. Key points selected on a Palmprint image help in extracting and determining position and size (fixed) of square.

Published by: The Mattingley Publishing Co., Inc.

March-April 2020
ISSN: 0193-4120 Page No. 26444 - 26454

Make sure that the detected ROI from acquired image is available on all palmprints and possesses all realistic features having fixed ROI size. The Palmprint ROI detection is as shown in Figure 4.

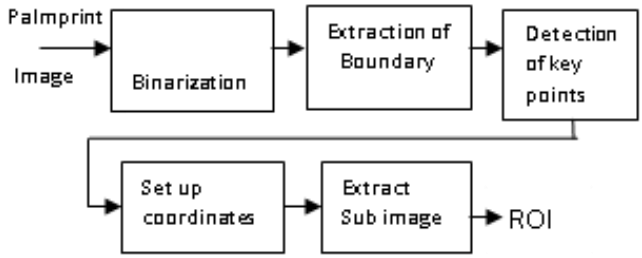

Fig. 4. Block diagram of ROI detection for palmprint

Image Binarization

Histogram of the acquired image is analyzed to determine the local minima i.e. threshold (T_p), which forms the basis for conversion of acquired image into a binary image using mathematical calculations, represented in eq (2) and eq (3),

$$BO(x,y)=1 \quad if\ I(x,y)\otimes F(x,y)\geq T_p \tag{2}$$

$$BO(x,y)=0 \quad if\ I(x,y)\otimes F(x,y),<T_p \tag{3}$$

where $BO(x,y)$ - binary image, $I(x;\ y)$ - acquired image, $F(x,y)$ - low-pass filter, $\otimes$ convolution operator. Threshold value T_p is calculated using Otsu's algorithm.

Boundary Extraction

Irrelevant small objects are removed from output binary image by eroding with structure element of 3x3 ones'. Boundary of one pixel thickness is then extracted using Sobel edge operator. This boundary is then scanned row-wise to get the boundary pixels. Reference point P_1(first left-down pixel) and P_2 (first left-up pixel) of the output binary image are identified using boundary pixels.

Detecting Key Point

Detection of key points is obtained by tracing the external boundary pixels of palmprint from reference point P_1 (moving clockwise) and reference point P_2 (moving anti-clockwise). A graph stating distance between boundaries points and extreme points of image is generated for all boundary pixels. The notch point between little and ring finger is detected as local maxima K_1, and another local maxima K_2 is detected as the notch between index and middle finger are located on graph.

Establish a Coordinate System

K_m is mid-point on the line $K_1$and K_2, A line is drawn from K_m perpendicular to K_1K_2. A rectangle parallel to line joining K_1K_2 of fixed size is drawn on palmprint, which represents region of the interest (ROI) for the given Palmprint.

V. FEATURE EXTRACTION

For individual biometrics modality features like Gabor, Radon, Radon-Gabor, Ridgelet, FPLBP, and TPLBP are used are discussed in brief as given below.

Gabor Transform

Name after by Dennis Gabor (Gabor, 1946), the Gabor filter is a non-orthogonal linear filter. The single dimension Gabor filter extended to two dimensions filter by Daugman [20], the equations are as given in eq (4) and eq (5),

$$F_e(x,y)=\frac{1}{2\pi\sigma_x\sigma_y}e^{-\frac{1}{2}(\frac{x^2}{2\sigma_x}+\frac{y^2}{2\sigma_y})}\ cos(\ 2\pi\omega_0 x+2\pi\omega_0 y) \tag{4}$$

$$F_o(x,y)=\frac{1}{2\pi\sigma_x\sigma_y}e^{-\frac{1}{2}(\frac{x^2}{2\sigma_x}+\frac{y^2}{2\sigma_y})}\ sin(\ 2\pi\omega_0 x+2\pi\omega_0 y) \tag{5}$$

where, $(\omega_0 x,\omega_0 y)$ - center frequency and (σ_x,σ_y) - spread of the filter.

Figure 5 and Figure 6 shows the images of the Gabor transform for different orientation such as θ= (0.0; 22.5; 45.0; 67.5; 90.0; 112.5; 135.0; 157.5), for 8 orientation, but we used 16 orientations in the experimentation. The Gabor filter used for images is basically a Gaussian with variances σ_x and σ_y along x and y -axes respectively.

Gabor filter is applied on ROI of sample in fixed number of orientations and is fused to reduce dimensionality giving filtered image. 16 oriented Gabber convolution filters are used in the present work which generated 16 outputs. The maximum

Published by: The Mattingley Publishing Co., Inc.

March-April 2020
ISSN: 0193-4120 Page No. 26444 - 26454

value obtained of pixel is considered for final output of image.

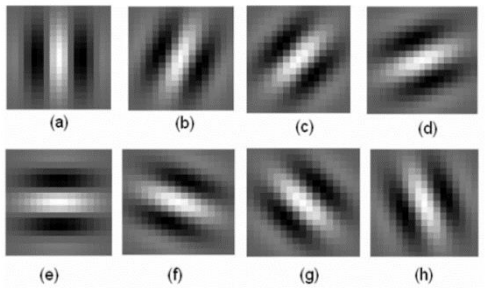

Fig 5. Typical Two-dimensional Gabor filter response with different orientation

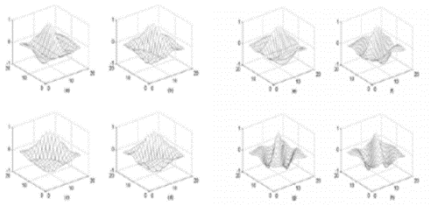

Fig. 6. Typical Three-dimensional structure of Gabor filter with eight orientation

Radon Transform:

Radon transform captures the directional features of an image because of its natural properties [21]. The two-dimensional Radon transform function $I(x,y)$ [22] in (s,θ) plane is defined by eq (6)

$$R(s,\theta)[I(x,y)] = \int_{-\infty}^{\infty}\int_{-\infty}^{\infty} I(x,y)\partial(s - x\cos\theta - y\sin\theta)dxdy \quad (6)$$

where, $\delta(.)$, Dirac function, $s \in (-\infty,+\infty)$, orthogonal distance of line with respect to origin and $\theta \in [0,\pi]$ - angle formed by vector as illustrated in Figure 7.

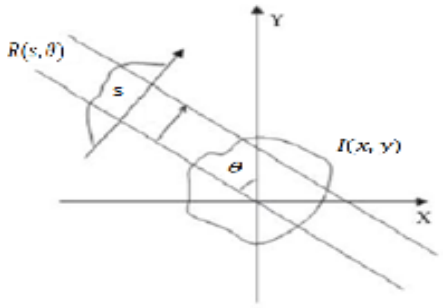

Fig. 7. Radon transforms projection.

Ridgelet [23]

One dimensional wavelet transformation performed on radon transform projections of an image leads to determination of Ridgelet [24]. 1-D wavelet transform applied on radon projections defines Ridgelet transform, and is given in eq. (7).

$$RID_f(a,b,\theta) = \int_R \Psi_{a,b},\theta(x)I(x)\,dx \quad (7)$$

where, θ-angle of orientation, a-indexes scale of Ridgelet, b- location of Ridgelet, and Ridgelet $\Psi_{a,b,\theta}(x)$ in 2-Dimension are demarcated from a wavelet function in 1-Dimension $\Psi(x)$ as eq.(8),

$$\Psi_{a,b,\theta}(x) = a^{-1/2}\Psi((x_1\cos\theta + x_2\sin\theta - b)/a) \quad (8)$$

B-spline wavelet is adopted since it is found to be the optimum amongst others other wavelets. **Radon-Gabor [14]**

Radon-Gabor transform is used since Radon transform is not affected due to rotation and improves low frequency component and Gabor transform provides multiple directions and improves low frequency features into multiple directions. Multiple orientation features are derived by blending Gabor decomposition in different orientations of Radon space. Eight images derived from the eight orientations are fused to obtain one template. The resultant equations for Radon-Gabor transform are as defined by eq. (9), (10), (11)

$$G[R(\tau(\tau,\eta)f(y)] = G[\iint f(x,y)\delta(x,x\cos\ \eta\eta - \sin\ \eta\eta)\ \delta x\delta y\ ] \quad (9)$$

$$= \iint_{-\infty}^{\infty} e^{-\pi(\tau-t_1)^2}e^{-j2\pi f_1\tau}e^{-\pi(\eta-t_2)^2}e^{-j2\pi f_2\eta} \iint_{-\infty}^{\infty} f(x,y)\delta(\tau - x\cos\eta - y\sin\eta)\delta x\delta y\ \delta\tau\delta\eta \quad (10)$$

$$= \iint_{-\infty}^{\infty}\iint_{-\infty}^{\infty} e^{-\pi(\tau-t_1)^2}e^{-j2\pi f_1\tau}e^{-\pi(\eta-t_2)^2}e^{-j2\pi f_2\eta} f(x,y)\delta(\tau - x\cos\eta - y\sin\eta)\delta x\delta y\delta\tau\delta\eta \quad (11)$$

where $\delta(.)$- dirac function, $\tau \in (-\infty,+\infty)$ - orthogonal distance from origin and $\eta \in [0,\pi]$ - angle build by vector, R(.) defines the Radon transform and G(.) defines the Gabor transform.

Three-Patch LBP Codes (TPLBP)[25]:

Three-Patch LBP is given by the eq (12)

Published by: The Mattingley Publishing Co., Inc.

March-April 2020
ISSN: 0193-4120 Page No. 26444 - 26454

$$TPLBP_{r,S,\omega,\alpha}(p) = \sum_i^S f(d(C_i, C_p) - d(C_{i+\alpha \bmod S,}\, C_p))2^i \quad (12)$$

where C_i and $C_{i+\alpha \bmod S}$, dual patches along ring and C_p, central patch. Distance of two patches is given by $d(..)$ and function f is given by eq (13)

$$f(x) = \begin{cases} 1 \; if \; x \geq \tau \\ 0 \; if \; x < \tau \end{cases} \quad (13)$$

Four-Patch LBP Codes(FPLBP)[25]:

Four-Patch LBP is given by the eq (14)

$$FPLBP_{r1,r2,,S,\omega,\alpha}(p) = \sum_i^{S/2} f(d(C_{1i}, C_{2,i+\alpha \bmod S}) - d(C_{1,i+S/2,}\, C_{2,i+\frac{S}{2}+\alpha \bmod S}))2^i \quad (14)$$

VI. BIOMETRIC FUSION

Fused feature vectors (FFV) are formed for every individual subject by fusion of face and palmprint feature vector. FFV mean and FFV weighted sum method for fusion are proposed. The pre-requisite for feature fusion is same dimensions for all the modalities.

Fused Feature Vector Mean (FFVM)

Let fv^{fv} be the m dimensional feature vector and n modalities of biometrics entities. Then the Fused Feature Vector Mean (FFVM) is given by eq (15).

$$\text{FFVM(i)} = \left[\frac{\left(\sum_{j=1}^{n} fv_{j,i}\right)}{n}\right] \; \forall i = 1,2,\ldots,m \quad (15)$$

The interpretation of FFVM(i) is the average value of n modalities in ith dimension.

Fused Feature Vector Weighted Sum (FFVW)

All feature vectors do not contribute equally to recognize the pattern and hence weighted sum is proposed over FFVM. Dominant feature are given higher weights as compared to other un-important features using weighted vectors. The FFVW is computed as in eq (16).

$$\text{FFVW(i)} = \sum_{j=1}^{n} \left(fv_{j,i} \times wg(j)\right) \; \forall i = 1,2,\ldots,m \quad (16)$$

where, $wg(j)$ is weight assigned to jth biometric modality.

Confidence based approach (SSIM):

SSIM compares structural exactness amongst 2 images and yields an index in the range of -1 (exactly different) to 1 (exactly same). It is given in eq (17)

$$\text{SSIM(x,y)} = \frac{(2\mu_x\mu_y + c1)(2\sigma_{xy} + c2)}{(\mu_x^2 + \mu_y^2 + c1)(\sigma_x^2 + \sigma_y^2 + c2)} \quad (17)$$

where, μ_x mean of x, μ_y mean of y, σ_x^2 variance of x, σ_y^2 variance of y, $c1 = (k_1 l)^2$, $c2 = (k_2 l)^2$ variables stabilize division with a weaker denominator , l dynamic range of the pixel values , $k_1 = 0.01$ and $k_2 = 0.03$ by default

VII. EXPERIMENTATION AND RESULTS

Experimentation was performed on the databases of Face images and Palm print images and fusion of features of Face images and Palm print images is performed as discussed in following section.

Face Recognition

For experimentation faces94 [26], faces95 [26], faces96 [26], FERET [27] and FRGC [28] databases are used for face modality. The Face 94 and Face 96 data set holds 151 subjects and 20 samples per subject, whereas Face95 is composed of 72 subjects and for each subject 20 samples. FERET consist of 13000 thousands images of 1500 different subjects. For experimentation 250 subjects with 6 sample of each are selected. FRGC database consist of 50,000 samples of around 4000 subjects. For experimentation 100 subjects with 6 sample of each are selected. One sample per subject is applied for training and other samples are considered for testing the algorithm. DCT, Gabor, Radon, Ridgelet, Radon Gabor, HOG, FPLBP and TPLBP are used in face recognition. Experimentation performed on the five face databases for calculation of accuracy with considering one training sample. The obtained results are mentioned in Table 1. It is observed that FPLBP and TPLBP features give the accuracy better than other features.

Palm print Recognition

The palm print dataset used for experimentation is PolyU and IIT Delhi (IITD) [29] data set. The PolyU

Published by: The Mattingley Publishing Co., Inc.

March-April 2020
ISSN: 0193-4120 Page No. 26444 - 26454

[30] database contains 386 Subjects with Right and Left Palm and 10 sample of each palm. IITD contains 230 subjects and 6 samples of each hand (right- and left-hand palm print) of the subjects are captured. Thus, total of 12×230 samples are available. The palm print ROI is extracted from the whole print. Training set is composed of one sample image of left hand of each subject and remaining samples are given for testing for both datasets. The obtained results are mentioned in Table 2. It is observed that TPLBP and FPLBP features give the accuracy better than other features. The accuracy for IITD database is more by at least 10% compared to PolyU database

Fusion of Face and Palm Print

The database for multimodal biometrics system is formed by considering first subject face image from face database and first subject Palmprint image from palmprint database and so on for rest of subjects. Face and palm print modality features vectors are fused using two proposed methods FFVM and FFVW, as described in (17) and (18), respectively. The obtained results for fusion are mentioned in Table 3-6 . Peak results are as shown in bold figures in the result tables.

The results shown in Table 2 shows identification accuracy of multimodal biometric system is highest for TPLBP features. The identification accuracy is 100% for TPLBP feature set for face 95, Face96 and FERET databases, and gives the better accuracy for Face94 and FRGC database.

The identification accuracy is 100% for TPLBP feature set for Face94, Face 95, Face96, and FERET databases, and gives the better accuracy for FRGC database. It is observed that the accuracy for FFVM get improved by 0.45% compared to the FFVW algorithm.

The results shown in Table 5 shows identification accuracy of multimodal biometric system is improved compared to individual biometrics. The identification accuracy is 99.73% for FPLBP feature set for Face 94 databases, 92.89% for TPLBP feature for FERET and FRGC database, and gives the better accuracy for Face95, Face96 using the Gabor features for multimodal Biometric system using FFVW algorithm.

The results shown in Table 6 shows identification accuracy of multimodal biometric system is highest for TPLBP features. The identification accuracy is 99.33% for FPLBP feature set for Face 94 databases, more than 92.89% for TPLBP feature for Face95, Face96, FERET and FRGC database for multimodal Biometric system using FFVM algorithm.

As per experimentation, it is observed that highest accuracy of 100% is obtained using TPLBP (FFVM) features for Face94, Face95, Face 96, FERET and IIT Delhi data set. The maximum accuracies obtained using single and multimodal features and the comparison is as shown in Table 7. The identification accuracy for IITD palmprint database and Face dataset gives the 100% accuracy but the accuracy is lesser for PolyU database with Face databases.

Table 1. Accuracy with Face databases

Algorithm	Face 94	Face 95	Face 96	FERET	FRGC
Gabor	93.57	72.29	62.733	59.53	83
DCT	64.73	34.65	23.44	32.53	60.83
Radon	97.31	84.37	80.89	64.86	87.66
Radon-Gabor	97.51	84.72	68.37	55.73	84.50
HOG	95.26	68.88	49.70	44.06	75.83
Ridgelet	98.11	86.25	80.39	71.06	90
FPLBP	99.07	90.83	78.34	72.53	94.16
TPLBP	98.24	87.63	71.95	74.60	95.33

Published by: The Mattingley Publishing Co., Inc.

March-April 2020
ISSN: 0193-4120 Page No. 26444 - 26454

Table 2. Accuracy with Palmprint databases

Algorithm	IITD	PolyU
Gabor	73.91	40.44
DCT	75	46.70
Radon	86.81	72.25
Radon-Gabor	76.66	59.09
HOG	81.66	62.56
Ridgelet	89.71	75.95
FPLBP	92.10	73.08
TPLBP	92.75	82.56

Table 3. Fusion with IITD FFVW

Algorithm	Face 94	Face 95	Face 96	FERET	FRGC
Gabor	98.34	96.99	98.34	83.76	83.83
DCT	86.86	62.73	68.21	75.79	68.33
Radon	98.67	97.68	95.69	89.13	91.66
Radon-Gabor	99.22	96.29	89.84	67.39	88.50
HOG	97.79	86.80	76.71	56.01	76
Ridgelet	99.55	97.22	95.14	90.79	93.33
FPLBP	**99.88**	100	99.55	99.20	96.33
TPLBP	99.55	**100**	**100**	**100**	**98.83**

Table 4. Fusion with IITD FFVM

Algorithm	Face 94	Face 95	Face 96	FERET	FRGC
Gabor	96.02	93.75	96.02	81.37	80.66
DCT	68.32	44.67	63.24	76.95	65.83
Radon	98.34	92.12	91.72	88.69	86.66
Radon-Gabor	99.11	96.06	92.05	77.46	90.66
HOG	87.85	76.38	74.06	71.44	73.33
Ridgelet	99.22	96.52	95.03	92.10	93.66
FPLBP	100	100	100	100	96.50
TPLBP	**100**	**100**	**100**	**100**	**97.50**

Table 5. Fusion with PolyU FFVW

Algorithm	Face 94	Face 95	Face 96	FERET	FRGC
Gabor	97.01	**96.52**	**97.01**	63.84	63.84
DCT	84.50	64.30	56.62	42.89	42.89
Radon	98.74	88.33	88.67	70.07	70.07
Radon-Gabor	98.80	88.19	82.05	67.46	67.46
HOG	98.94	58.61	58.41	51.15	51.15

Published by: The Mattingley Publishing Co., Inc.

March-April 2020
ISSN: 0193-4120 Page No. 26444 - 26454

Ridgelet	99.27	91.25	90.99	61.59	61.59
FPLBP	**99.73**	91.94	88.54	79.78	79.78
TPLBP	98.80	91.80	89.40	**92.89**	**92.89**

Table 6. Fusion with PolyU FFVM

Algorithm	Face 94	Face 95	Face 96	FERET	FRGC
Gabor	90.46	90.97	90.46	56.81	56.81
DCT	83.90	61.11	53.31	42.89	47.89
Radon	98.60	89.98	90.59	76.88	76.88
Radon-Gabor	98.47	89.16	84.17	72.60	72.60
HOG	97.35	40.83	61.19	59.13	59.13
Ridgelet	98.80	90.96	90.92	28.98	28.98
FPLBP	**99.33**	91.94	90.52	85.72	85.72
TPLBP	98.60	**93.33**	**93.04**	**92.89**	**94.71**

Table 7. Comparison of maximum accuracies for single and multimodal features

Maximum Accuracy	Face 94	Face95	Face96	FERET	FRGC	Palm IITD	Palm PolyU
Single modality	99.07	90.83	80.89	74.60	95.33	92.75	82.56
Fusion IITD FFVW	99.88	100	100	100	**98.83**		
Fusion IITD FFVM	**100**	**100**	**100**	**100**	97.50		
Fusion PolyU FFVW	99.27	96.52	97.01	92.89	92.89		
Fusion PolyU FFVM	99.33	93.33	93.04	92.89	94.71		

VIII. CONCLUSION

In this presented work of identification, identification rate is 100% for FERET Face and IITD palmprint images. It is observed maximum accuracy of 74.60% for Face modality using TPLBP features with SSIM method.

The maximum accuracy obtained for palm print is 92.75% using TPLBP and SSIM. As per our comparison of single and multi-modal fusion technique, we obtained 25.40% more accuracy than single face modality and 7.25% improvement over single palm print modality.

The best combination for fusion was found to be TPLBP with Fused Feature Vector Mean using SSIM, for face and palm print.

REFERENCES

[1] A. K. Jain, A. Ross and S. Pankanti, “Biometrics: A Tool for Information Security”, IEEE Transactions on Information Forensics and Security, vol. 1, no. 2, (2006), pp. 125-143.

[2] A. K. Jain, A. Ross and S. Prabhakar, “An Introduction to Biometric Recognition”, IEEE Transactions on Circuits and Systems

Published by: The Mattingley Publishing Co., Inc.

for Video Technology, vol. 14, no. 1,(2004), pp. 4-20.

[3] A. Ross and Anil Jain, "Information Fusion in Biometrics", Pattern Recognition Letters, vol. 24, Issue 13,(2003) pp. 2115-2125.

[4] K. Nandakumar, Y. Chen, S. C. Dass and A. K. Jain, "Likelihood Ratio Based Biometric Score Fusion," IEEE Transactions on Pattern Analysis and Machine Intelligence, vol. 30, no. 2,(2008) pp. 342-347.

[5] Abhishek Nagar; Karthik Nandakumar ; Anil K. Jain, "Multibiometric Cryptosystems Based on Feature-Level Fusion," IEEE Transactions on Information Forensics and Security, vol. 7, Issue 1,(2012), PP.255-268.

[6] Ajay Kumar, Sumit Shekhar, "Personal Identification using Rank-level Fusion," IEEE Trans. Systems, Man, and Cybernetics: Part C, vol. 41, no. 5, (2011), pp. 743-752.

[7] Padma Polash Paul, Marina L. Gavrilova ; Reda Alhajj, "Decision Fusion for Multimodal Biometrics Using Social Network Analysis," IEEE Transactions on Systems, Man, and Cybernetics: Systems, vol. 44, Issue: 11, (2014).

[8] Zhou Wang, A. C. Bovik, H. R. Sheikh and E. P. Simoncelli, "Image quality assessment: from error visibility to structural similarity," IEEE Transactions on Image Processing, vol.13, no.4, (2004), pp.600-612.

[9] S. Veluchamy, L.R. Karlmarx, "System for multimodal biometric recognition based on finger knuckle and finger vein using feature-level fusion and k-support vector machine classifier," IET Biometrics, vol. 6, Issue: 3, 5, (2017), pp. 232 – 242.

[10] Yong-Fang Yaoa, Xiao-Yuan Jingb, Hau-San Wong, "Face and palmprint feature level fusion for single sample biometrics recognition," Neurocomputing, vol.70, (2007), pp. 1582–1586.

[11] R Raghavendra, B Dorizzi, Ashok Rao, Hemantha Kumar, "Designing efficient fusion schemes for multimodal biometric systems using face and palmprint," Pattern Recognition, vol. 44,(2011), pp.1076-1088.

[12] Xiao-Yuan Jing, Yong-Fang Yao, David Zhang, Jin-Yu Yang, Miao Li, "Face and palmprint pixel level fusion and kernel DCV-RBF classifier for small sample biometric recognition," Pattern recognition, Vol 40, (2007), pp.3209-3224.

[13] Yong Xu, David Zhang , Jing-Yu Yang, "A feature extraction method for use with bimodal biometrics," Pattern Recognition, vol.43, (2010),pp.1106-1115.

[14] Milind E Rane, Umesh Bhadade, "Multimodal System using Radon-Gabor Transform," International Conference on Energy, Communication, Data Analytics and Soft Computing (ICECDS), India, (2017).

[15] Satyajit Kautkar, Rahulkumar Koche, Tushar Keskar, Aniket Pande, Milind Rane, Gary A. Atkinson, "Face Recognition Based on Ridgelet Transforms," ICEBT 2010, Procedia Computer Science 2, pp.35–43, (2010).

[16] Bruce Lindbloom, "RGB Working Space Information" 2014. URL: http://www.brucelindbloom.com/WorkingSpaceInfo.html.

[17] R. A. Hummel: Image Enhancement by Histogram Transformation. Computer Graphics and Image Processing 6 (1977).

[18] K. Zuiderveld, "Contrast Limited Adaptive Histogram Equalization," Graphics Gems IV, Academic Press, (1994) , pp 474-485.

[19] Milind E. Rane, Umesh S Bhadade, "Comparative Study of ROI Extraction of Palmprint," IJCSN International Journal of Computer Science and Network, Volume 5, Issue 2, (2016), pp.251-255.

[20] Daugman J "Gabor wavelets and statistical pattern recognition," The Handbook of Brain Theory and Neural Networks, 2nd ed., MIT Press, (2002) , pp 457 -463.

[21] E. Magli, G. Olmo, L. Lo Presti, "Pattern recognition by means of the Radon transform

and the continuous wavelet transform", Signal Processing vol. 73, (1999), pp.277 - 289,.

[22] G. Beylkin, "Discrete Radon transform," IEEE Transactions Acoustics, Speech Signal Process. ASSP, vol. 35(2), (1987), pp. 162 - 171.

[23] Minh N. Do, Martin Vetterli, "The Finite Ridgelet Transform for Image Representation," IEEE Transactions on Image Processing, vol.12, Issue 1, (2003), pp.16- 28,.

[24] Candès, Emmanuel J., and David L. Donoho, "Ridgelets: a key to higher-dimensional intermittency?" Philosophical Transactions of the Royal Society of London A: Mathematical, Physical and Engineering Sciences (1999).

[25] Lior Wolf, Tal Hassner, and Yaniv Taigman. Descriptor Based Methods in the Wild. Faces in Real-Life Images workshop at the European Conference on Computer Vision (ECCV), Marseille, (2008).

[26] SPACEK, L. "Computer Vision Science Research Projects," 2008 [Online]. Available: http://cswww.essex.ac.uk/mv/allfaces/index.html

[27] P.J. Phillips, H. Moon, S.A. Rizvi, P.J. Rauss, The FERET evaluation methodology for face recognition algorithms, IEEE Trans. Pattern Anal. Machine Intell. Vol.22, no.10, (2000), pp. 1090–1104.

[28] P. Jonathon Phillips, The Face Recognition Grand Challenge (FRGC) ver2.0 Database.

[29] Ajay Kumar, "Incorporating Cohort Information for Reliable Palmprint Authentication," Proc. ICVGIP, Bhubneshwar, India, (2008), pp. 583-590.

[30] The Hong Kong Polytechnic University, PolyU Palmprint Database, [Online]. Available: http:// www.comp.polyu.edu.hk/ biometrics.